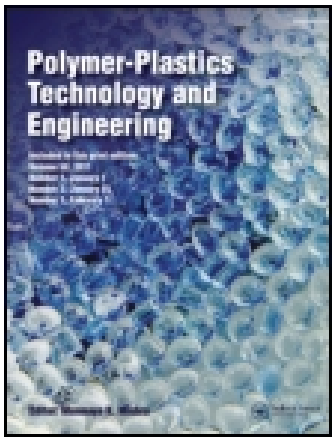

Polymer-Plastics Technology and Engineering
Publication details, including instructions for authors and subscription information:
http://www.tandfonline.com/loi/lpte20

Chitosan and Poly(Methyl Methacrylate-Co-Butyl Methacrylate) Bioblends: A Compatibility Study

Nelson Luis G. D. Souza [a] , Humberto M. Brandão [b] & Luiz Fernando C. de Oliveira [a]
[a] NEEM - Núcleo de Espectroscopia and Estrutura Molecular, Departamento de Química , Universidade Federal de Juiz de Fora , Juiz de Fora , MG , Brazil
[b] Empresa Brasileira de Pesquisa Agropecuária, Centro Nacional de Pesquisa de Gado de Leite , Juiz de Fora , MG , Brasil
Accepted author version posted online: 26 Nov 2013.Published online: 14 Feb 2014.

Polymer-Plastics Technology and Engineering, 53: 319–326, 2014

ISSN: 0360-2559 print/1525-6111 online
DOI: 10.1080/03602559.2013.844240

Taylor & Francis
Taylor & Francis Group

Chitosan and Poly(Methyl Methacrylate-Co-Butyl Methacrylate) Bioblends: A Compatibility Study

Nelson Luis G. D. Souza[1], Humberto M. Brandão[2], and Luiz Fernando C. de Oliveira[1]

[1]*NEEM – Núcleo de Espectroscopia and Estrutura Molecular, Departamento de Química, Universidade Federal de Juiz de Fora, Juiz de Fora, MG, Brazil*
[2]*Empresa Brasileira de Pesquisa Agropecuária, Centro Nacional de Pesquisa de Gado de Leite, Juiz de Fora, MG, Brasil*

Chitosan/poly(methyl methacrylate-co-butyl methacrylate) (PMMA-co-BMA) blends were prepared via a solution blending method in the presence of formic acid. The compatibility of the bioblends was studied by different methods, such as Fourier transform infrared and Raman spectroscopy, micro-Raman imaging, thermogravimetric analyses, differential scanning calorimetry and scanning electron microscopic analysis. According to the obtained results, it has been concluded that the PMMA-co-BMA/chitosan bioblends are compatible in all the studied compositions. Specific interactions between carbonyl and methyl groups of the PMMA-co-BMA structure and methyl, amine and amide groups of chitosan are responsible for the observed compatibility.

Keywords Chitosan; Compatibility; Poly(methyl methacrylate-co-butyl methacrylate); Polymer bioblends; Supramolecular interactions

INTRODUCTION

Concerns about environmental problems such as global warming, pollution of natural resources, renewable energy use and cost of synthetic polymers have motivated an intense research of sustainable polymer systems where at least one component is biodegradable or biobased[1]. The commercial importance of polymers also have increased the need of discover of new materials with specific properties and applications; for this purpose new polymers have been synthesized and chemical modifications in conventional polymers have also been proposed, but these methods are more complicated[2,3]. However, the mixture of two or more polymers, giving rise to a polymer blend, seems to be an economical method to obtain new polymeric materials with desirable properties, without the need of synthesizes specialized polymer systems[4,5].

Polymer blends containing at least one biodegradable polymer component are referred to as bioblends[6], which have properties of the natural component (good mechanical properties, easy processability, low production and transformation costs and biocompatibility), typical for biopolymers[7].The polymeric bioblends have been used as matrices for delivery systems[8], membranes[9] and materials for agriculture[10]. The final properties of the polymer blends depend on the properties of their components, the composition and especially the compatibility of polymers; for most polymer blends is caused by specific interactions[11], such as dipole-dipole, ion-dipole and hydrogen bonding interactions[12]. In some cases, due to the synergistic effect, the mixtures present better properties than their individual components[13–15]. In literature there are investigations involving the mixture of chitosan with different polymers[16], such as poly(vinyl alcohol)[17], poly(N-vinyl pyrrolidone)[18], poly(ethylene oxide)[19], cellulose[20] and its derivatives[21], among others; however, there are no reports describing a polymer blend containing chitosan and poly(methylmethacrylate-co-butyl methacrylate).

This investigation purposes the preparation and characterization of films from a polymeric bioblend composed by chitosan and poly (methyl methacrylate-co-butylmethacrylate). The compatibility of the bioblends has been investigated by means of Fourier transform infrared spectroscopy, Raman spectroscopy, micro-Raman imaging, thermogravimetric analyses, differential scanning calorimetry and scanning electron microscopic analysis, in order to evaluate the compatibility as well as the supramolecular interactions between these two polymers.

MATERIALS AND METHODS

Materials

Chitosan (medium molecular weight) and poly(methyl methacrylate-co-butyl methacrylate) ($M_w = 75{,}000$) polymers were purchased from Sigma Aldrich and were used

Address correspondence to Luiz Fernando C. de Oliveira, NEEM – Núcleo de Espectroscopia and Estrutura Molecular, Departamento de Química, Universidade Federal de Juiz de Fora, Juiz de Fora, MG, 36036-900, Brazil. E-mail: luiz.oliveira@ufjf.edu.br

Color versions of one or more of the figures in the article can be found online at www.tandfonline.com/lpte.

without any further purification. Formic acid 85% as purchased from Vetec, and used as a solvent without further purification.

Bioblend Preparation

Polymer bioblends were prepared using the solvent evaporation technique. Five different solutions of chitosan and poly(methyl methacrylate-co-butyl methacrylate (PMMA-co-BMA) in acid formic were prepared by mixing both polymers in the weight ratios of 0/100, 25/75, 50/50, 75/25 and 100/0 of chitosan and PMMA-co-BMA, respectively. The solutions were left under stirring for 24 h, and after that were transferred to Petri dishes for solvent evaporation; the bioblends were collected as transparent cast films.

Fourier Transform Infrared Spectroscopy

Fourier transform infrared (FTIR) spectra of polymer bioblends were obtained in a Bomem FTIR (Fourier Transform Infrared Spectroscopy) spectrometer model MB102 (Canada) in the 4000–400 cm^{-1} region. The chitosan samples were prepared using KBr as support, with a resolution of 4 cm^{-1} and 64 scan accumulations.

Raman Spectroscopy

Raman measurements were performed on a Bruker RFS 100 spectrophotometer (Germany) excited with an Nd^{+3}/YAG laser operating at 1064 nm, equipped with a CCD detector cooled with liquid nitrogen and a spectral resolution of 2 cm^{-1}. An average of 1024 scans were collected with a laser power of 200 mW directed at the sample. All spectra were collected at least twice to ensure reproduction of wavenumber positions and intensities.

Micro-Raman Imaging

The measurements were performed on Bruker RFS 100 spectrophotometer (Germany) excited with a Nd^{+3}/YAG laser operating at 1064 nm, equipped with a CCD detector cooled with liquid nitrogen and a spectral resolution of 4 cm^{-1}. The Raman image was acquired using a 40× optical lens. For this analysis were used 49 points using a laser power of 300 mW and 1024 accumulations for each point. For this analysis we reviewed the band at 1383 cm^{-1} to visualize chitosan and at 812 cm^{-1} to visualize PMMA-co-BMA.

Thermogravimetric Analyses

Thermogravimetric analyses (TG) were performed in a Shimadzu TG-60 instrument under nitrogen atmosphere in a flow of 50.0 mL/min, with a heating rate of 10°C/min, from 25 to 900°C.

Differential Scanning Calorimetry

Differential scanning calorimetry analyses (DSC) were carried out in the Shimadzu DSC-60 calorimeter (Japan). The samples analysis were performed at a heating rate of 20°C/min under nitrogen atmosphere at a purge speed of 50 mL/min, as specified in the ASTM D 3418–03 standard test description.

Scanning Electron Microscopic Analysis

The scanning electron microscopic (SEM) micrographs of the bioblend samples were obtained under high resolution (magnification: 20,000×, 10 kV) using a scanning electron microscope FEI Quanta 400 with a system of chemical microanalysis by energy dispersive (EDS) coupled Bruker 800 Quantax to analyze the samples were analyzed deposited on silicon plates and coated with silver.

RESULTS AND DISCUSSION

Vibrational Spectral Study

It is known that if two polymers originate an incompatible blend, there should be no appreciable change in the vibrational spectrum of the blend, when compared to the spectrum of each one of the isolated components. However, if the polymers are compatible, interactions in the blends will result in clear differences in the spectra[22]. In this sense, infrared spectroscopy (FT-IR) is a useful technique in studying polymer blends, especially blends with hydrogen bonding interactions[23,24].

The infrared spectra of the samples are shown in Figure 1, and the main vibrational bands are reported in Table 1, together with a tentative assignment based on literature[25–30]. Analyzing the bands related to chitosan is possible to verify alterations at 1640, 1592 and 1350 cm^{-1}, assigned to the ν(C=O) from amide group, $\delta(NH_2)$ and ν(C-N) from amine group, respectively. The band at 1640 cm^{-1} shifts to 1668 cm^{-1} and becomes more intense than the band at 1592 cm^{-1} in the spectrum of the 75 chitosan/25 PMMA-co-BMA and 50 chitosan/50 PMMA-co-BMA bioblends. The band at 1592 cm^{-1} shifts to 1635 cm^{-1} in the 75 chitosan/25 PMMA-co-BMA and a shoulder appears at 1618 for 50 chitosan/50 PMMA-co-BMA bioblend. On the other hand, the band at 1350 cm^{-1} can be observed at lower wavenumbers with increasing the chitosan ratio[31].

All these observed perturbations on the vibrational modes strongly suggest the existence of interactions between the polymers, probably due to the presence of the amine and amide groups present in the chitosan structure[16,32]. In relation to PMMA-co-BMA is possible to verify changes in the bands on the vibrational modes of methyl and ester groups. There is an increase of the relative band intensity at 1243 cm^{-1} when compared to the one at 1273 cm^{-1}, and the appearance of a shoulder at 1262 cm^{-1}; the bands at 1243 and 1273 cm^{-1} are assigned to the ν_s(C-C-O) mode.

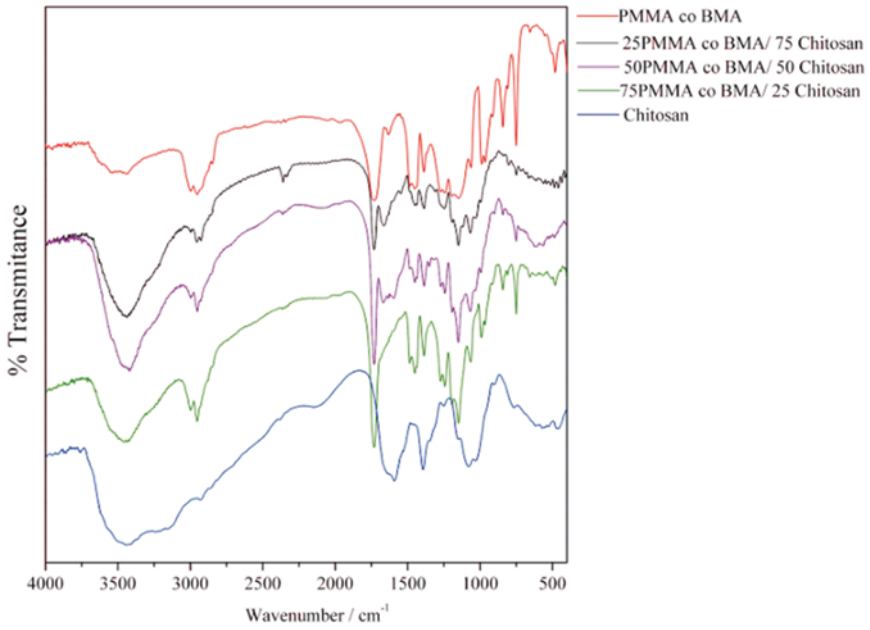

FIG. 1. Infrared absorption spectra of the samples indicated.

In the 1100–1200 cm^{-1} region, where the ν_a(C-O-C) mode can be seen, is clear the appearance of a shoulder at 1119 cm^{-1} in the band at 1146 cm^{-1}, which becomes more intense than the band at 1194 cm^{-1}. All the observed spectroscopic changes strongly suggest the formation of hydrogen bonds through the ester groups, since there is

TABLE 1
Main infrared and Raman wavenumber values (in cm^{-1}) of the indicated samples

PMMA-co-BMA			Chitosan		
Infrared	Raman	Tentative assignment	Infrared	Raman	Tentative assignment
2996	3000	ν_a(C-H) of O-CH_3 and C-CH_3	3731–2999		ν(OH) + υ(NH)
2950	2951	ν_s(C-H) of O-CH_3 and C-CH_3 + ν_a(CH_2)	2930/2859	2936/2893	ν(CH_2)
2927		ν(C-H)			
2847	2844	ν_a(CH_2)	1640	1720	ν(C=O) amide
1731	1729	ν(C=O)	1592	895	δ(NH_2)
1486	1485/1450	δ(CH_2)	1393	1383	δ(CH_3) in amide
1450		δ_a(C-H) of CH_3	1347		ν(C-N) amide
1387/1366	1390	δ_s(C-H) of CH_3	1250		δ(OH) out of plane
1437		δ_s(C-H) of O-CH_3	1150		ν(C-O-C) from β(1–4) bond
1273/1243		ν_s(C–C–O)	1078	1118	ν(C-O-C) glucosyl ring
	1239	ν(C–C)			
1194/1146	1123	ν_a(C–O-C)	903		ν(C-O-C) from β(1–4) bond
1063	983/966	ν(C–C)			
	1062	methylene wagging			
989		δ(C-H) of O-CH_3			
964		δ(C-H) of C-CH_3			
843		δ(CH_2)			
809	812	ν(CC_4)			
	601	δ(C-C=O)			
	482/365	δ(CC_4)			

the formation of a shoulder at lower wavenumber, according to previous reports for other similar bioblends[33,34]. There is also a change in position and intensity for the bands in the 3100–2800 cm^{-1} region, assigned to the C-H stretching modes, as well as a shift of the band at 989 cm^{-1}, assigned to the (C-H) deformation mode of O-CH_3 group, to a higher wavenumber value. Once again, all the changes in the spectra are indicative of the presence of interactions between the polymers, mainly involving the methyl group of the PMMA-co-BMA structure[35].

The Raman spectra of the samples are shown in Figure 2, and the main vibrational bands are also reported in Table 1, together with a tentative assignment based on literature[27,28,36,37]. Differences between the spectra of pure polymers and their mixtures can be observed in the Raman spectra. The bands at 1383 and 895 cm^{-1}, assigned respectively to $\delta(CH_3)$ of amide and $\delta(NH_2)$ for the chitosan polymer, are shifted to higher wavenumbers, and the bands at 1123 and 811 cm^{-1} referring to the PMMA-co-BMA and assigned respectively to ν_a(C–O-C) and $\nu(CC_4)$ are shifted to lower wavenumbers.

Raman features at 1720 and 1729 cm^{-1}, assigned to ν(C=O) amide for the chitosan and ν(C=O) for the PMMA-co-BMA, respectively, present a shift in the spectra of the bioblends, to a wavenumber value which is intermediary to those of the pure polymers. As discussed before for the infrared data, the changes observed in the bioblends Raman spectra are indicative of the presence of intermolecular interactions between the methyl and ester groups of PMMA-co-BMA and methyl, and the amine and amide groups of chitosan. Previous similar works investigating a polymer with a chemical structure analogous to PMMA-co-BMA by means of Raman spectroscopy, have also showed a relationship between the formation of hydrogen bonds and the compatibility of the polymers[28,33].

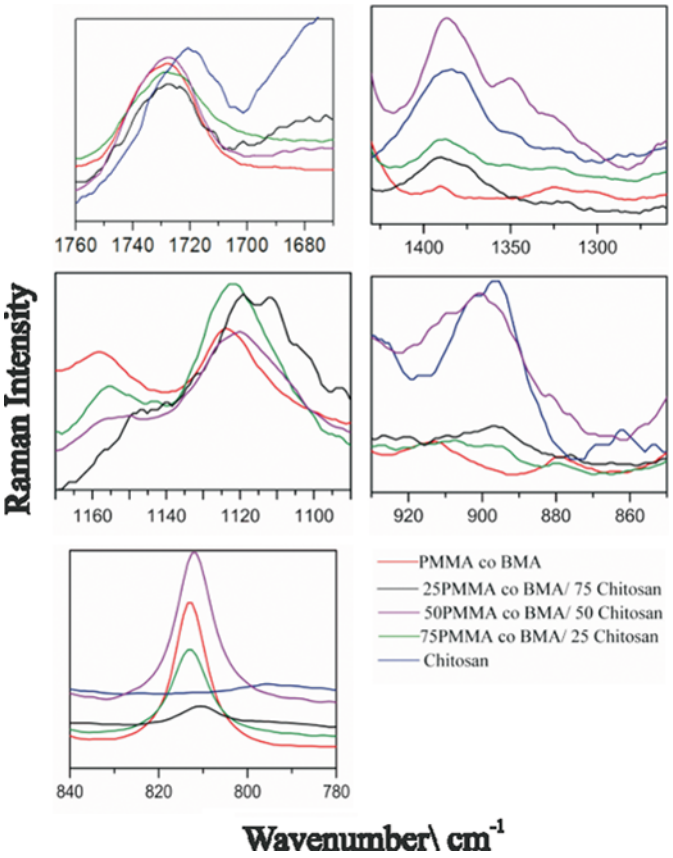

FIG. 2. Raman spectra excited at 1064 nm of the samples indicated.

Micro-Raman Imaging

The Raman image analysis is applied to the study of spatial distribution of molecular species of polymer bioblends[38]. The optical and Raman image of the samples are showed in Figure 3. The Raman band at 1383 cm^{-1} is suited for visualizing chitosan, while the band at 812 cm^{-1} is suited for visualizing PMMA-co-BMA. These bands are assigned to the $\delta(CH_3)$ mode of amide group from chitosan and ν(C-C_4) from PMMA-co-BMA, respectively. It can be observed in Figure 3 the presence of both bands in all the analyzed polymeric surfaces; this result indicates the homogeneity in the polymeric bioblend, which is related to its compatibility between the polymers[39]. The same results can be achieved with the analysis of other Raman bands, such as the ones at 600 (for PMMA-co-BMA) and 1118 cm^{-1} (for Chitosan). It is worth of mention the very low number of investigations concerning the Raman mapping of polymer surfaces, indicating a gap in information on this specific subject.

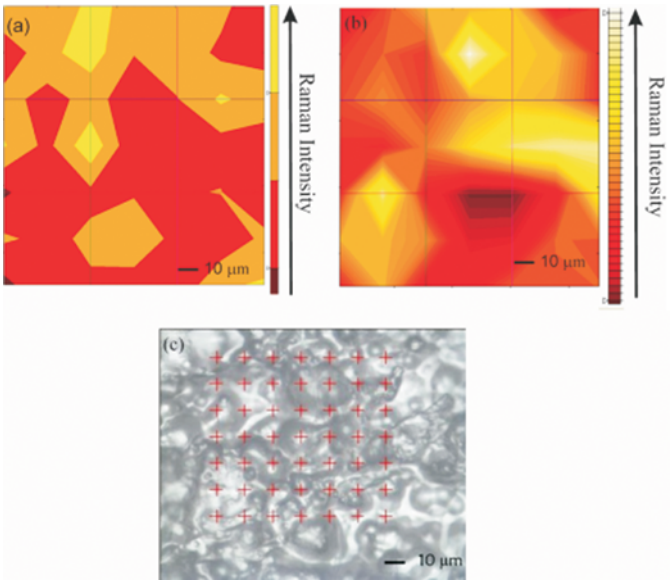

FIG. 3. Micro-Raman Imaging of the 50 PMMA-co-BMA/50 Chitosan sample.

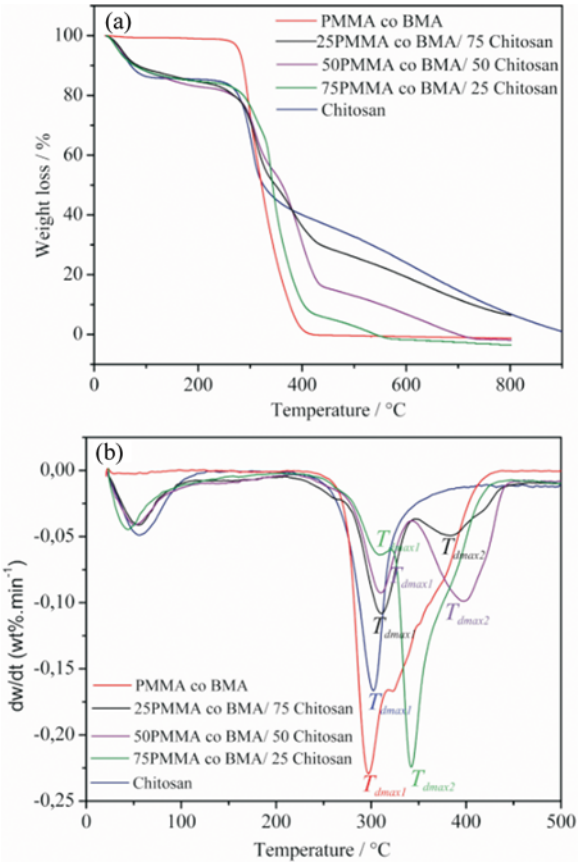

FIG. 4. TGA curves of PMMA-co-BMA, chitosan and PMMA-co-BMA/chitosan blends (a) and DTG curves of PMMA-co-BMA, chitosan and PMMA-co-BMA/chitosan blends.

TG Analysis

Figure 4(a) displays the thermogravimetric curves of PMMA-co-BMA, chitosan and PMMA-co-BMA/chitosan bioblends. It can be observed that PMMA-co-BMA polymer degrades completely in a single stage, pronouncedly beginning at *ca.* 250°C and ending at 430°C. On the other hand, a three-stage weight loss was recorded for the chitosan membrane, as previously described[40].

All polymeric bioblends showed a three-stage degradation behavior. The first stage, between 40 and 200°C, should be associated with the loss of water in chitosan and the elimination of the possible trace amounts of formic acid left inside the bioblends. The second and the third thermal events are related to the degradation of chitosan and PMMA-co-BMA. The TG curves of the polymeric bioblends show a different behavior when compared to the pure polymers. This difference is verified by analyzing the initial decomposition temperature (T_{onset}) of the polymer bioblends[41], which are summarized in Table 1. For the polymeric bioblends is possible to observe an increase of T_{onset} with the increase of PMMA-co-BMA ratio, being indicative of an improvement of the thermal stability. This shift to higher temperatures indicates the existence of some supramolecular interactions between the polymer components in the bioblend, and not only a mechanical mixture[42].

The TG curves are better analyzed by means of the derivative thermal analysis; the DTG data are depicted in Figure 4(b) and the collected data are summarized in Table 2. Each temperature value for the peaks in Figure 4(b) is marked as T_{dmax}, which corresponds to the maximum degradation rate. All polymeric bioblends exhibit two peaks of fast thermal degradation, being typical for each one of the components. To make further comparisons among the bioblends with different thermal degradation peak positions, the peaks at a lower and higher temperature are designated as T_{dmax1} and T_{dmax2}, respectively.

In general, in a binary bioblend system, an improved thermal stability would be achieved for the component with a lower T_{dmax1} if the measured T_{dmax1} shifts toward the higher T_{dmax1} of the other component; this shift can be understood as due to the several supramolecular

TABLE 2
Thermal data of Chitosan, PMMA-co-BMA and their blends in different ratios

Composition	TG Tonset (°C)	DTG Tdmax1 (°C)	DTG Tdmax2 (°C)	DSC Experimental Tg (°C)	DSC Theoretical Tg (°C)
Chitosan	280	302		37	
75 PMMA-co-BMA/25 chitosan	292	310	384	73	73
50 PMMA-co-BMA/50 chitosan	292	310	397	63	55
25 PMMA-co-BMA/75 chitosan	288	309	342		44
PMMA-co-BMA	281	297		107	

interactions between both components[42]. In the present case, there are evidences showing that the measured T_{dmax1} of chitosan component significantly moves towards the T_{dmax2} of PMMA-co-BMA component. This shift is not related to the increase of PMMA-co-BMA concentration, but seems to be related to the degree of the strong supramolecular interactions between both polymers.

Differential Scanning Calorimetry

According to literature, a polymeric blend can be considered compatible, only if a new T_g (glass transition temperature) can be observed between the original T_{gs} of the components. On the other hand, they are partially compatible only if the resulting blends would have two T_{gs} related to each component, but with different values when compared to the pure polymers[43]. The theoretical T_g values can be predicted using the Fox equation[44]:

$$\frac{1}{T_g} = \frac{X_1}{T_{g1}} + \frac{X_2}{T_{g2}} \quad (1)$$

where X_1, X_2, T_{g1}, and T_{g2} are the weight fractions and glass transition temperatures of polymers 1 and 2, respectively[44].

The DSC curves obtained for the different polymers and the bioblends are presented in Figure 5, whereas the values of experimental and theoretical T_{gs} are displayed in Table 2. The DSC curves corresponding to pure polymers present a single change in slope at 37°C for the chitosan and at 107°C to the PMMA-co-BMA. In the case of the 25 chitosan/75 PMMA-co-BMA and 50 chitosan/50 PMMA-co-BMA bioblends, a single transition can be observed occurring at a temperature that is intermediate between those of the pure components, that moves towards values by increasing the PMMA-co-BMA ratio.

It is straightforward to note that these values are in good agreement with the theoretically expected. In the DSC curve of 75 chitosan/25 PMMA-co-BMA bioblend an intermediate transition temperature was not observed, but also did not present the glass transition event related to the pure polymers. The lack of the glass transition for this bioblend can be due to a small change in its heat capacity, which is probably too small to be detected by DSC technique[45]. The results obtained through DSC strongly suggest a compatibility between the polymers, which is probably due to the existence of intermolecular interactions between the individual polymers[46].

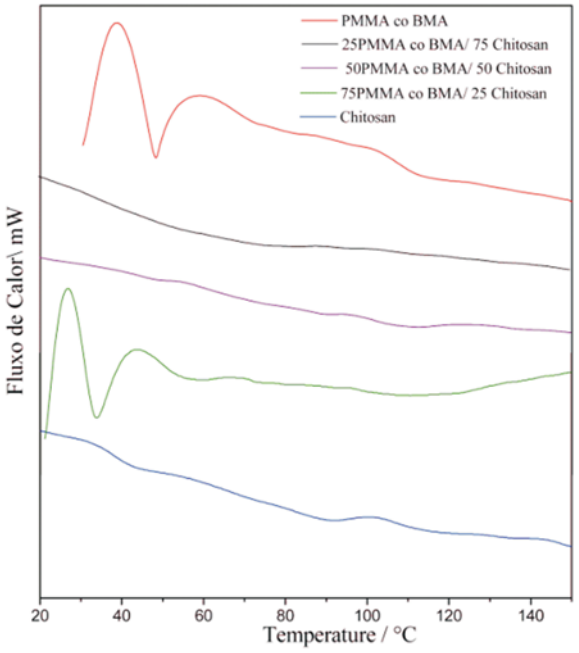

FIG. 5. DSC curves of the samples indicated.

Scanning Electron Microscopic Analysis

Scanning electron microscopic analysis (SEM) is a common qualitative technique for visual identification and estimation of bioblend compatibility[47]. Figure 6 shows the SEM images of the individual polymers as well the polymeric bioblends, where is possible to observe

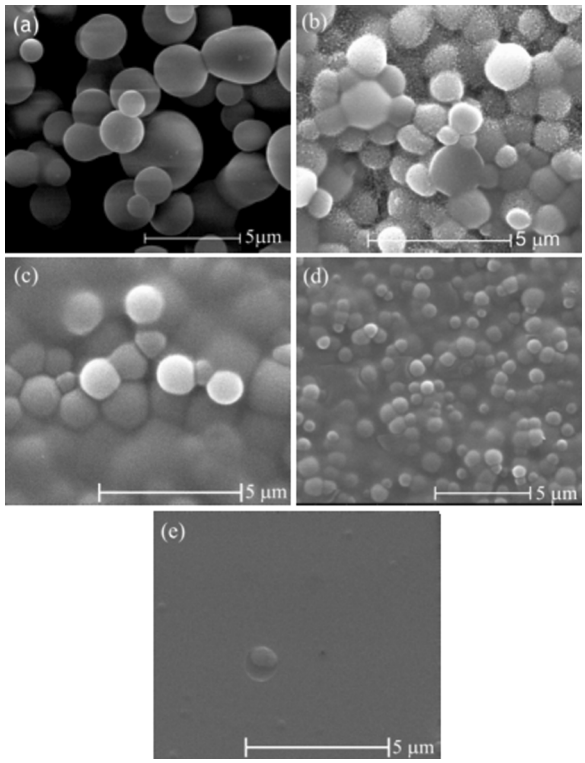

FIG. 6. SEM images of PMMA-co-BMA (a), 75 PMMA-co-BMA/25 Chitosan (b), 50 PMMA-co-BMA/50 Chitosan (c), 25 PMMA-co-BMA/75 Chitosan (d) and Chitosan (e).

a change in the morphology of the bioblends when the chitosan concentration increases. Figure 6(a) corresponds to the SEM image of PMMA-co-BMA, and Figure 6(e) corresponds to the pure chitosan; Figures 6(b), (c) and (d) correspond to the different bioblends: 25, 50 and 75 chitosan. Analysis of all the SEM images show clearly a decrease in the size of the particles when the concentration of PMMA-co-BMA decreases, and there is a good homogeneity for all the bioblends at least in the magnification of the measurement, and no obvious phase separation boundary could be seen. This last comment also strongly suggest a good compatibility between the two polymers, which is in a good agreement with literature[48].

CONCLUSIONS

The compatibility of chitosan/PMMA-co-BMA bioblends has been studied by methods such as infrared and Raman spectroscopy, micro-Raman imaging, thermogravimetric analyses, differential scanning calorimetry and scanning electron microscopic analysis. According to all the aforementioned methods, chitosan and PMMA-co-BMA give rise to compatible bioblends. Through the spectroscopic analysis of the polymer bioblends it was found that the compatibility of these materials is due to specific supramolecular interactions, involving the carbonyl and methyl groups of PMMA-co-BMA and the methyl, amide and amine groups of chitosan.

The use of SEM and micro-Raman images indicates homogeneity of surface morphology of the polymer bioblends. DSC confirmed that the compatibility of the bioblends due to presence of only one glass transition temperature. Finally, TGA results show that the formation of polymeric bioblends increases the thermal stability of the new materials. The present results show that the production of new polymer bioblends obtained from a natural and a synthetic polymer in different concentrations originate new properties, such as mechanical properties, which are closely related to the degree of compatibility between the individual polymers.

FUNDING

This research was supported by CNPq, CAPES and FAPEMIG (Brazilian agencies). This work is a collaboration research project of members of the Rede Mineira de Química (RQ-MG) supported by FAPEMIG (Project: REDE-113/10).

REFERENCES

1. Akhlaghi, S.; Sharif, A.; Kalaee, M.; Manafi, M. Miscibility and thermal behavior of poly(vinyl chloride)/feather keratin blends. J. Appl. Polym. Sci. **2011**, *121* (6), 3252–3261.
2. Gagnon, K.D.; Lenz, R.W.; Farris, R.J.; Fuller, R.C. Chemical modification of bacterial elastomers: 2. Sulfur vulcanization. Polymer **1994**, *35* (20), 4368–4375.
3. Stadler, R.; Auschra, C.; Beckmann, J.; Krappe, U.; Voight-Martin, I.; Leibler, L. Morphology and thermodynamics of symmetric poly(A-block-B-block-C) triblock copolymers. Macromolecules **1995**, *28* (9), 3080–3097.
4. Zhou, Y.; Yin, B.; Li, L.-P.; Yang, M.-B.; Feng, J.-M. Characterization of PP/EPDM/HDPE ternary blends: The role of two EPDM with different viscosity and processing method. Polym. Plast. Technol. Eng. **2012**, *51* (10), 983–990.
5. Zhu, G.; Wang, F.; Tan, H.; Gao, Q.; Liu, Y. Properties study of poly(L-lactic acid)/polyurethane-blend film. Polym. Plast. Technol. Eng. **2012**, *51* (15), 1562–1566.
6. Girma, B.; Abdellatif, M.; Sherald, H.G.; Rogers, E.H.-O.k.; Craig, C.C. Compatibility study in poly(tetramethyleneadipate-co-terephthalate)/polystyrene bioblends. J. Appl. Polym. Sci. **2008**, *110* (5), 2932–2941.
7. Cascone, M.G.; Barbani, N.; Cristallini, C.; Giusti, P.; Ciardelli, G.; Lazzeri, L. Bioartificial polymeric materials based on polysaccharides. J. Biomater. Sci.-Polym. Ed. **2001**, *12* (3), 267–281.
8. Cascone, M.G.; Sim, B.; Sandra, D. Blends of synthetic and natural polymers as drug delivery systems for growth hormone. Biomaterials **1995**, *16* (7), 569–574.
9. Yang, J.M.; Su, W.Y.; Leu, T.L.; Yang, M.C. Evaluation of chitosan/PVA blended hydrogel membranes. J. Membrane Sci. **2004**, *236* (1–2), 39–51.
10. Chiellini, E.; Cinelli, P.; Imam, S.H.; Mao, L. Composite films based on biorelated agro-industrial waste and poly(vinyl alcohol). Preparation and mechanical properties characterization. Biomacromolecules **2001**, *2* (3), 1029–1037.
11. Sato, T.; Endo, M.; Shiomi, T.; Imai, K. UCST behaviour for high-molecular-weight polymer blends and estimation of segmental χ parameters from their miscibility. Polymer **1996**, *37* (11), 2131–2136.
12. Parashar, P.; Ramakrishna, K.; Ramaprasad A.T. A study on compatibility of polymer blends of polystyrene/poly(4-vinylpyridine). J. Appl. Polym. Sci. **2011**, *120* (3), 1729–1735.
13. Chuayjuljit, S.; Chantanaprasartporn, A.; Wiparchon, J.; Boonmahitthisud, A. Physical properties of plasticized poly(vinyl chloride) blended with poly(methyl methacrylate) nanoparticles synthesized by differential microemulsion polymerization. Int. J. Polym. Mat. Polym. Biomater. **2012**, *62* (5), 247–251.
14. Hong, X.; Nie, G.; Lin, Z.; Rong, J. Structure and properties of PPO/PP blends compatibilized by triblock copolymer SEBS and SEPS. Polym. Plast. Technol. Eng. **2012**, *51* (10), 971–976.
15. Kucharczyk, P.; Otgonzu, O.; Kitano, T.; Gregorova, A.; Kreuh, D.; Cvelbar, U.; Sedlarik, V.; Saha, P. Correlation of morphology and viscoelastic properties of partially biodegradable polymer blends based on polyamide 6 and polylactide copolyester. Polym. Plast. Technol. Eng. **2012**, *51* (14), 1432–1442.
16. Yin, J.; Luo, K.; Chen, X.; Khutoryanskiy, V.V. Miscibility studies of the blends of chitosan with some cellulose ethers. Carbohydr. Polym. **2006**, *63* (2), 238–244.
17. Mucha, M.; Pawlak, A. Thermal analysis of chitosan and its blends. Thermochim. Acta **2005**, *427* (1–2), 69–76.
18. Sakurai, K.; Maegawa, T.; Takahashi, T. Glass transition temperature of chitosan and miscibility of chitosan/poly(N-vinyl pyrrolidone) blends. Polymer **2000**, *41* (19), 7051–7056.
19. Amiji, M.M. Permeability and blood compatibility properties of chitosan-poly(ethylene oxide) blend membranes for haemodialysis. Biomaterials **1995**, *16* (8), 593–599.
20. Twu, Y.-K.; Huang, H.-I.; Chang, S.-Y.; Wang, S.-L. Preparation and sorption activity of chitosan/cellulose blend beads. Carbohydr. Polym. **2003**, *54* (4), 425–430.
21. Pawlak, A.; Mucha, M. Thermogravimetric and FTIR studies of chitosan blends. Thermochim. Acta **2003**, *396* (1–2), 153–166.
22. Dong, J.; Fredericks, P.M.; George, G.A. Studies of the structure and thermal degradation of poly(vinyl chloride)—poly (N-vinyl-2-pyrrolidone) blends by using Raman and FTIR emission spectroscopy. Polym. Degrad. Stabil. **1997**, *58* (1–2), 159–169.

23. Wu, C.; Wu, Y.; Zhang, R. Miscibility of phenoxy polymer/poly (methyl acrylate-co-methyl methacrylate) blends. Eur. Polym. J. **1998**, *34* (9), 1261–1263.
24. Zhu, G.; Gao, Q.; Wang, F.; Zhang, H. Structure and performance of poly(vinyl alcohol)/poly(γ-benzyl l-glutamate) blend membranes. Int. J. Polym. Mat. Polym. Biomater. **2011**, *60* (9), 720–728.
25. Buckles, J.M.; Garay, J.C.; Kaufman, D.J.; Layson, A.R.; Columbia, M.R. Specular-reflectance IR spectroscopy of polymethylmethacrylate thin films: An experiment for the undergraduate instrumental analysis course. J. Chem. Educ. **1998**, *3* (3), 1–11.
26. Willis, H.A.; Zichy, V.J.I.; Hendra, P.J. The laser-Raman and infrared spectra of poly(methyl methacrylate). Polymer **1969**, *10*, 737–746.
27. Souza, N.L.G.D.; Brandão, H.M.; de Oliveira, L.F.C. Spectroscopic and thermogravimetric study of chitosan after incubation in bovine rumen. J. Mol. Struct. **2011**, *1005* (1–3), 186–191.
28. Matsushita, A.; Ren, Y.; Matsukawa, K.; Inoue, H.; Minami, Y.; Noda, I.; Ozaki, Y. Two-dimensional Fourier-transform Raman and near-infrared correlation spectroscopy studies of poly(methyl methacrylate) blends: 1. Immiscible blends of poly(methyl methacrylate) and atactic polystyrene. Vib. Spectrosc. **2000**, *24* (2), 171–180.
29. Ramesh, S.; Leen, K.H.; Kumutha, K.; Arof, A.K. FTIR studies of PVC/PMMA blend based polymer electrolytes. Spectrochim. Acta Pt. A **2007**, *66* (4–5), 1237–1242.
30. Costa-Júnior, E.S.; Barbosa-Stancioli, E.F.; Mansur, A.A.P.; Vasconcelos, W.L.; Mansur, H.S. Preparation and characterization of chitosan/poly(vinyl alcohol) chemically crosslinked blends for biomedical applications. Carbohydr. Polym. **2009**, *76* (3), 472–481.
31. Silva, S.S.; Goodfellow, B.J.; Benesch, J.; Rocha, J.; Mano, J.F.; Reis, R.L. Morphology and miscibility of chitosan/soy protein blended membranes. Carbohydr. Polym. **2007**, *70* (1), 25–31.
32. Castro, C.; Gargallo, L.; Radic', D.; Mondragon, I.; Kortaberria, G. Blends of chitosan and poly(sodium-4-styrene sulphonate). Compatibilization by lysine and glutamic acid. Carbohydr. Polym. **2010**, *82* (3), 795–801.
33. Dong, J.; Ozaki, Y. FTIR and FT-Raman studies of partially miscible poly(methyl methacrylate)/poly(4-vinylphenol) blends in solid states. Macromolecules **1997**, *30* (2), 286–292.
34. Song, M.; Long, F. Miscibility in blends of poly(vinyl acetate) with poly(methyl methacrylate) studied by FTIR and DSC. Eur. Polym. J. **1991**, *27* (9), 983–986.
35. Osman, Z.; Ansor, N.; Chew, K.; Kamarulzaman, N. Infrared and conductivity studies on blends of PMMA/PEO based polymer electrolytes. International Conference on Functional Materials and Devices, Malaysia, June, **2005**, *11* (5), 431–435.
36. Orrego, C.E.; Salgado, N.; Valencia, J.S.; Giraldo, G.I.; Giraldo, O.H.; Cardona, C.A. Novel chitosan membranes as support for lipases immobilization: Characterization aspects. Carbohydr. Polym. **2010**, *79* (1), 9–16.
37. Synytsya, A.; Blafková, P.; Synytsya, A.; Čopíková, J.; Spěváček, J.; Uher, M. Conjugation of kojic acid with chitosan. Carbohydr. Polym. **2008**, *72* (1), 21–31.
38. Garton, A.; Batchelder, D.N.; Cheng, C. Raman microscopy of polymer blends. Appl. Spectrosc. **1993**, *47* (7), 922–927.
39. Schaeberle, M.D.; Karakatsanis, C.G.; Lau, C.J.; Treado, P.J. Raman chemical imaging: Noninvasive visualization of polymer blend architecture. Anal. Chem. **1995**, *67* (23), 4316–4321.
40. Neto, C.G.T.; Giacometti, J.A.; Job, A.E.; Ferreira, F.C.; Fonseca, J.L.C.; Pereira, M.R. Thermal analysis of chitosan based networks. Carbohydr. Polym. **2005**, *62* (2), 97–103.
41. Hadj-Hamou, A.S.; Habi, A.; Djadoun, S. Thermal and FTIR analysis of the miscibility and phase behaviour of poly (isobutyl methacrylate-co-4-vinylpyridine)/poly (styrene-co-acrylic acid) systems. Thermochim. Acta **2010**, *497* (1–2), 117–123.
42. Katarzyna, L. Miscibility and thermal stability of poly(vinyl alcohol)/chitosan mixtures. Thermochim. Acta **2009**, *493* (1–2), 42–48.
43. Cameron, N.; Cowie, J.M.G.; Ferguson, R.; Gómez Ribelles, J.L.; Más Estellés, J. Transition from miscibility to immiscibility in blends of poly(methyl methacrylate) and styrene–acrylonitrile copolymers with varying copolymer composition: a DSC study. Eur. Polym. J. **2002**, *38* (3), 597–605.
44. M'Bareck, C.O.; Nguyen, Q.T.; Metayer, M.; Saiter, J.M.; Garda, M.R. Poly (acrylic acid) and poly (sodium styrenesulfonate) compatibility by Fourier transform infrared and differential scanning calorimetry. Polymer **2004**, *45* (12), 4181–4187.
45. Lee, S.J.; Kim, S.S.; Lee Y.M. Interpenetrating polymer network hydrogels based on poly(ethylene glycol) macromer and chitosan. Carbohydr. Polym. **2000**, *41* (2), 197–205.
46. Aouachria, K.; Belhaneche-Bensemra, N. Miscibility of PVC/PMMA blends by vicat softening temperature, viscometry, DSC and FTIR analysis. Polym. Test. **2006**, *25* (8), 1101–1108.
47. Reddy, K.S.; Prabhakar, M.N.; Reddy, V.N.; Sathyamaiah, G.; Maruthi, Y.; Subha, M.C.S.; Chowdoji Rao, K. Miscibility studies of hydroxypropyl cellulose/poly(vinyl pyrrolidone) in dilute solutions and solid state. J. Appl. Polym. Sci. **2012**, *125* (3), 2289–2296.
48. Choudhary, P.; Mohanty, S.; Nayak, S.K.; Unnikrishnan, L. Poly (L-lactide)/polypropylene blends: Evaluation of mechanical, thermal, and morphological characteristics. J. Appl. Polym. Sci. **2011**, *121* (6), 3223–3237.